Biogeosciences Discuss., doi:10.5194/bg-2016-367, 2016
Manuscript under review for journal Biogeosciences
Published: 7 September 2016
© Author(s) 2016. CC-BY 3.0 License.

Biogeosciences Discussions
Open Access
EGU

The origin of methane in the East Siberian Arctic Shelf unraveled with triple isotope analysis

[1,2]Célia J. Sapart*, [3,4]Natalia Shakhova, [3,4,5]Igor Semiletov, [1,6]Joachim Jansen, [7]Sönke Szidat, [5]Denis Kosmach, [5]Oleg Dudarev, [1]Carina van der Veen, [8]Matthias Egger, [9]Valentine Sergienko, [5]Anatoly Salyuk, [10]Vladimir Tumskoy, [2]Jean-Louis Tison and [1]Thomas Röckmann.

[1]Institute for Marine and Atmospheric research Utrecht (IMAU), Utrecht University, Princetonplein 5, 3584CC Utrecht, The Netherlands.

[2]Laboratoire de glaciologie, Universtié Libre de Bruxelles (ULB), Avenue Roosevelt 50, 1050 Brussels, Belgium.

[3]University Alaska Fairbanks, International Arctic Research Center, 930 Koyukuk Drive, Fairbanks, USA, 99775.

[4]Tomsk Polytechnic University, 30 Prospect Lenina, Tomsk, Russia.

[5]Russian Academy of Sciences, Far Eastern Branch, V.I. Il'ichov Pacific Ocenological Institute, 43 Baltiyskaya street, Vladivostok 690041.

[6]Department of Geological Sciences and Bolin Centre for Climate Research, Stockholm University, Frescativägen 8, SE 114 18, Stockholm, Sweden.

[7]Department of Chemistry and Biochemistry & Oeschger Centre for Climate Change Research, University of Bern, Freiestrasse 3, CH-3012 Bern, Switzerland.

[8]Department of Earth Sciences - Geochemistry, Utrecht University, Princetonplein 9, 3584CC Utrecht, The Netherlands.

[9]Russian Academy of Sciences, Far Eastern Branch, Institute of Chemistry, 159 Prospect 100-letiya Vladivostoka, Vladivostok 690022.

[10]Moscow State University, 1 Leninskie Gori, 119991, Moscow, Russia.

Abstract

Methane (CH_4) is a strong greenhouse gas emitted by human activity and natural processes that are highly sensitive to climate change. The Arctic Ocean, especially the East Siberian Arctic Shelf (ESAS) overlays large areas of subsea permafrost that is degrading. The release of large amount of CH_4 originally stored or formed there could create a strong positive climate feedback. Large scale CH_4 super-saturation has been observed in the ESAS waters, pointing to leakages of CH_4 through the sea floor and possibly to the atmosphere, but the origin of this gas is still debated.

Here, we present CH_4 concentration and triple isotope data analyzed on gas extracted from sediment and water sampled over the shallow ESAS from 2007 to 2013. We find high concentrations (up to 500µM) of CH_4 in the pore water of the partially thawed subsea permafrost of this region. For all sediment cores, both hydrogen and carbon CH_4 isotope data reveal the predominant presence of CH_4 that is not of thermogenic/natural gas origin as

Biogeosciences Discuss., doi:10.5194/bg-2016-367, 2016
Manuscript under review for journal Biogeosciences
Published: 7 September 2016
© Author(s) 2016. CC-BY 3.0 License.

it has long been thought, but resultant from microbial CH_4 formation using as primary substrate glacial water and old organic matter preserved in the subsea permafrost or below. Radiocarbon data demonstrate that the CH_4 present in the ESAS sediment is of Pleistocene age or older, but a small contribution of highly ^{14}C-enriched CH_4, from unknown origin, prohibits precise age determination for one sediment core and in the water column. Our data suggest that at locations where bubble plumes have been observed, CH_4 can escape anaerobic oxidation in the surface sediment. CH_4 will then rapidly migrate through the very shallow water column of the ESAS to escape to the atmosphere generating a positive radiative feedback.

1.Introduction

The Arctic subsea permafrost harbors a very large active carbon pool of similar size as the terrestrial Siberian permafrost reservoir (Shakhova et al., 2010a). Between 12 and 5kyr Before Present (BP), the Holocene transgression (Bauch et al, 2001) submerged extensive parts of the Pleistocene age terrestrial permafrost in Northern Siberia, forming the very shallow ESAS (Romanovskii et al., 2005). As a result, the formerly terrestrial permafrost has been continuously exposed to increasing seawater temperatures, salt and anoxic conditions (Dimitrenko et al., 2011, Nicolsky et al., 2012) allowing the remobilization of carbon from the Pleistocene reservoirs. The four key mechanisms controlling the release of Pleistocene carbon from thawing subsea permafrost are gas hydrate degradation, thermokarst development, the deepening of the permafrost active layer and coastal erosion (e.g. Shakhova et al., 2005, 2009, 2010a,b, O'Connor et al., 2010, James et al., 2016). Holocene age carbon originating mainly from coastal erosion and riverine discharge (Charkin et al., 2011; Semiletov et al., 2011, 2012; Karlsson et al., 2011, 2016) has accumulated on the ESAS shelf and overlays the Pleistocene age sediment (Vonk et al., 2012, 2014 Feng et al., 2013).

Under specific conditions and depending on its type and quality (Schuur et al., 2013), the remobilized carbon can be used to produce CH_4, a strong greenhouse gas (IPCC, 2013). Biogenic CH_4 is produced by methanogenesis using as main substrates carbon dioxide (CO_2) and acetate according to the following reactions:

$$(CO_2 \text{ reduction})\ CO_2 + 4H_2 \rightarrow CH_4 + 2H_2O$$

$$(\text{Acetate fermentation})\ CH_3CO_2^- + H_2O \rightarrow CH_4 + HCO_3^-$$

In the deep Earth layers, thermogenic CH_4 can also be produced abiogenically by thermal degradation of organic matter (Schoell, 1988) and migrate towards the surface. A large part of the CH_4 formed in the seafloor is removed by anaerobic oxidation with seawater sulfate in the surface sediments (e.g. Reeburgh, 2007, Knittel and Boetius, 2009, Egger et al., 2015) or in the water column where CH_4 can be consumed by aerobic

Biogeosciences Discuss., doi:10.5194/bg-2016-367, 2016
Manuscript under review for journal Biogeosciences
Published: 7 September 2016
© Author(s) 2016. CC-BY 3.0 License.

methanotrophic bacteria under specific nutrient and redox conditions (e.g. Kessler et al., 2011, Mau et al., 2013, Steinle et al., 2015). Each type of CH_4 formation/removal pathway produces CH_4 with a characteristic isotopic signature ($\delta^{13}C$ and δD) depending on the isotopic composition of the substrate and the isotopic fractionation associated with the respective chemical reaction involved. Hence analyzing the isotopic composition of CH_4 in the sediment or in the water helps to unravel its formation/removal pathways (Whiticar, 1999, Quay et al., 1999).

At relatively high pressure and low temperature conditions in the seafloor, e.g. within the ESAS shelf and slope, CH_4 molecules can be stored as gas hydrate, i.e. encaged in frozen water molecules (e.g. Kvenvolden, 1988, Sloan et al., 2003, James et al., 2016). Below this gas hydrate stability zone, CH_4 occurs as free gas and can be advected towards the surface through faults in the sediment. Subsea permafrost has long been thought to play the role of a gas quasi-impermeable cap, preventing CH_4 to escape from seabed deposits (e.g. Soloviev et al., 1987, Bauch et al., 2001, Romanovskii et al., 2005, Shakhova et al., 2010a, Dmitrenko et al., 2011, Nicolsky et al., 2012). However, the warming of the ESAS bottom water, accelerated by the current decline in sea-ice coverage and the presence of geothermic activity in this region (Soloviev et al., 1987; Romanovskii et al., 2005) has largely degraded the ESAS subsea permafrost. This may cause a destabilization of the gas hydrate layers and provide more extensive pathways for gaseous and dissolved CH_4 to escape from the sediment to the atmosphere, e.g. when bubble plumes are released to the water column from the seabed (Shakhova et al., 2014, 2015) (for further discussion on gas transport processes within subsea permafrost see the SI Section 1). Shakhova et al., 2010b carried out a multi-year survey to measure CH_4 concentrations in the ESAS waters and showed that >80% of ESAS bottom waters and >50% of surface waters are supersaturated with CH_4 with respect to the atmosphere. Measured concentrations were anomalously high (up to 500 nM) compared to CH_4 values generally observed in oceans (~5 nM, Damm et al., 2008). Shakhova et al. (2010b, 2014, 2015) further observed vigorous bubbling at high concentration "hotspots" indicating that the water column CH_4 supersaturation must result from a strong source in the sediment.

To disentangle the origin(s) of this CH_4 anomaly, we measured CH_4 concentration, stable isotope composition and (on selected samples) radiocarbon content on sediment and water samples from several winter campaigns and summer cruises from 2007 to 2013 on the ESAS shelf and shelf edge. While stable isotope analyses help identify the chemical pathways involved in CH_4 removal and formation processes, radiocarbon measurements give information on the age of the CH_4 substrate the combination of the isotope information helps determine the possible origin(s) of this gas.

2.Method

2.1.Drilling and sediment sampling

Biogeosciences Discuss., doi:10.5194/bg-2016-367, 2016
Manuscript under review for journal Biogeosciences
Published: 7 September 2016
© Author(s) 2016. CC-BY 3.0 License.

Summer surface sediment drilling and water sampling campaigns were carried out from ships while the winter field campaigns were accomplished using an equipment caravan, which traveled over the sea ice to the drilling locations. In the latter case, casings were drilled through the fast ice into the seabed, allowing dry drilling using a rotary drill with 4 m casing with a newly built URB-4T drilling rig (made in 2011 by Vorovskii Factory for Drilling Equipment, Ekaterinburg, Russia). Thawed and frozen sediments for each core were subsampled straight after the drilling using ice screws for frozen samples and a heavy plastic syringe-like sampler for thawed samples at 20 cm vertical resolution.

2.2. Gas extraction and measurement in sediments

Sediment subsamples were immediately immersed in glass vials filled with a saturated sodium chloride solution to drive gases out of solution and capped with a septum for equilibrium in ultrasonic water bath at a temperature of 20°C. CH_4 concentrations in the headspace were measured immediately after equilibration with a SRI-8610c gas chromatograph, thermo-conductivity detector, a helium detector, a flame-ionization detector and two columns: molecular sieve 13X (6' x 1/8") and HayeSep D (6' x 1/8"). The amount of gas in the vials was calculated from headspace concentrations, gas pressure and solubility and the volume of liquid in the bottles following the method of Wiesenburg and Guinasso (1979). CH_4 concentrations are reported relative to sediment pore water volume, regardless of whether present as ice or water, based on calculated total sediment water content, bulk density and dry density (matrix or skeleton density) and sediment porosity. To estimate the sediment porosity (P_v), we calculated the density of the sediment skeleton (P_d) and density of the sediment mineral particles (P_s), so that $P_v = (P_s\text{-}P_d)/P_s$; where $P_d = P/(1+W_c)$; P is the total density of the sediment sample, which was calculated right upon sediment sample recovery by weighting the sample and measuring its volume. W_c is the sample moisture content (fraction of 1), calculated as the difference between the weight of the wet sediment sample and its dry weight. More details could be found in (Andersland and Ladanyi, 1994).

The stable isotope measurements were performed using a Continuous Flow Isotope Ratio Mass Spectrometry (CF-IRMS) system as described in Brass and Röckmann, 2010 and Sapart et al., 2011. Radiocarbon analyses could be performed only on the largest samples. In that case, CH_4 was preconcentrated and combusted to CO_2. The ^{14}C content of the CO_2 was measured by accelerator mass spectrometry (Szidat et al., 2014) using a specific gas inlet (Ruff et al., 2010).

2.3. Gas extraction and measurement from seawater samples

Water samples were collected directly from the Niskin bottles. Gas from seawater samples was extracted using a modified headspace vacuum-

Biogeosciences Discuss., doi:10.5194/bg-2016-367, 2016
Manuscript under review for journal Biogeosciences
Published: 7 September 2016
© Author(s) 2016. CC-BY 3.0 License.

ultrasonic degassing method (Schmitt et al., 1991, Lammers et al., 1994). The gas released was accumulated in an evacuated burette, to measure its volume and is then expanded into a smaller flask for storage, and analysed as described in Section 2.2.

3. Results and discussion

We present results of CH_4 concentration, stable isotope composition and (on selected samples) radiocarbon content on four shallow sediment cores (<3m), four deep sediment cores (ID-11, IID-13, IIID-13, VD-13) (down to 53m depth) and about fifty water samples from four coastal areas of the ESAS: the Lena Delta (LD), the Buor-Khaya Bay (BKB), the Dmitry Laptev Strait (DLS) and the Shelf Edge (SE) (Fig.1). All water and sediment sampling, except for the ID-11 core, was performed at hotspot sites, i.e., at locations where active gas bubbling from the seafloor and high concentrations of dissolved CH_4 were observed as discussed in Shakhova et al., 2010a. The location of core ID-11 is referred to as 'background site', where no gas bubbling was observed. Here, the core was thawed all the way down to 53m while the IID-13, IIID-13 and VD-13 cores were thawed down to 19, 17 and 12m, respectively. Note that sampling was continued through the deeper frozen sediment for the three latter cores to 30, 50 and 35m respectively. For more details on the lithology and sediment properties, see SI section 2 and Fig.S1.

3.2. CH_4 in the "deep" sediment

Depth profiles of CH_4 concentration, stable isotope composition ($\delta^{13}C$ and δD) and the radiocarbon content (in percent modern carbon, pmC) are presented in Fig.2. In both hotspot and background cores, CH_4 concentrations are far above values observed in the water column and CH_4 is strongly depleted in heavy isotopes in all sediment cores. CH_4 in the hotspot cores IID-13, IIID-13 and VD-13 is more depleted in δD and slightly more enriched in $\delta^{13}C$ than in the background core. These differences can be caused by the difference in lithology (Fig.S1), the heterogeneity in substrate availability (Karlsson et al., 2011, 2016, Tesi et al., 2014, 2016) at the different sampling locations, their distance from the coast and the depth of the gas formation, which will be discussed in detail below.

The expected stable isotope signatures of the three potential CH_4 formation pathways in sediment (Whiticar, 1999): CO_2 reduction, acetate fermentation and thermal degradation of organic matter are depicted together with our water and sediment stable isotope data in a dual isotope plot (Fig.3). Overall, the deep sediment core data (diamonds) fall in between the isotope source signatures of the two biogenic pathways: carbonate reduction and acetate fermentation. This could imply that CH_4 is formed by a mixture of both sources. However, salinity measurements along the deep sediment cores indicate the presence of interstitial seawater all the way down the cores. When the seawater sulfate enters the marine sediment (Henrichs and Reeburgh, 1987), it provides sulfate reducing bacteria with the electron

Biogeosciences Discuss., doi:10.5194/bg-2016-367, 2016
Manuscript under review for journal Biogeosciences
Published: 7 September 2016
© Author(s) 2016. CC-BY 3.0 License.

acceptor they need to outcompete methanogens for acetate (Lessner, 2009). This indicates that "in-situ" (i.e. at the depth where the samples were taken) acetoclastic CH_4 formation may be suppressed despite an abundance of organic material. CO_2 remains therefore the most likely non-competitive substrate for methanogens if "in-situ" formation would occur. Note that the presence of sulfate along the core might be expected to involve anaerobic oxidation of CH_4, but no significant enrichment in heavy isotopes in concert with concentration decrease is observed in the stable isotope profiles of the deep cores, except between 40 and 30m and between 4 and 0 m for the ID-11 core. This is further discussed in section 3.4.

Stable isotope measurements further support the notion that CH_4 is not produced at the sampling location using the infiltrated water, but migrates up from deeper layers. The exceptionally low δD values in the deep core sediment could be explained by the use of isotopically depleted water as substrate for CH_4 formation. Chanton et al, 2006 and Brosius et al., 2012 measured very low meltwater signatures ($\delta D(H_2O)$) of -135±25‰ and -220±30‰, respectively) in old Arctic permafrost (Fig. 4). We suggest that methanogens present in the thawing permafrost use and/or have used such depleted permafrost meltwater, unfrozen porewater or water from the hydraulic system (see SI, section 1) as a hydrogen source to form CH_4 with low δD values. Arctic modern seawater ($\delta D(H_2O)$ = -20‰ (Friedman et al., 1964)), infiltrating the marine sediment from above, is too enriched to explain the observed deuterium signature.

We conclude that the CH_4 present in the surface thawed subsea-permafrost is formed mainly biogenically by reduction of CO_2 in deeper (>53m) sediment layers where old, isotopically depleted meteoric (melt-)water is still present, or/and by acetate fermentation occurring at depth where no seawater sulfate is present. Our observations thus imply that CH_4 is not formed "in situ" but that it migrates from a deeper reservoir to the surface of the partially thawed ESAS subsea permafrost. This conclusion is supported by the observation that the vertical profiles - especially the stable isotope profiles - are relatively constant with depth. High CH_4 concentrations are also observed in frozen sediment showing that gas can migrate through permafrost even before it is completely thawed (see SI section 1 for further discussion on this topic).

The ^{14}C of CH_4 from the hotspot cores covers a range from 0.79 to 3.4pmC corresponding to a radiocarbon age of 26 to 39kyBP. This indicates a carbon substrate of Pleistocene age. For the ID-11 background core, ^{14}C values are unexpectedly high and vary from 87pmC (radiocarbon age=1kyBP) to 2367pmC, which represents a substantial enrichment above the natural background. The same applies for water samples from the SE. Note that levels close to 100pmC indicate modern values. Even samples that had been affected by the nuclear bomb testing in the 1950s and 1960s would show levels below 200pmC and ^{14}C values >200pmC cannot be caused by a known natural processes. As discussed in the SI section 3, local anthropogenic nuclear contribution is the most likely explanation for these elevated radiocarbon levels, however this contamination remains small in comparison to the main CH_4 source as it can be observed on the Keeling plot

Biogeosciences Discuss., doi:10.5194/bg-2016-367, 2016
Manuscript under review for journal Biogeosciences
Published: 7 September 2016
© Author(s) 2016. CC-BY 3.0 License.

(Keeling, 1961)(Fig. S2). Whereas this ^{14}C contamination complicates precise age determination using radiocarbon (considering that CH_4 present in the water is the result of a mixture of all possible sources), the ^{14}C values measured at the hotspot cores together with the very low δD values give strong evidences that CH_4 from old reservoirs (Pleistocene age or older) is being released there.

3.4. CH_4 in the surface sediment

The ID-11 background site was the only coring location where no active bubbling was observed from the surface sediment. Here, the top 5.8m consist of a thick silty-clay layer (Fig.S1) of marine origin as indicated by the higher salinity and silica concentrations, typical of a marine environment enriched in diatoms (Fig.5). The increase in sulfate concentration together with the strong CH_4 concentration decrease and the isotopic enrichment in both ^{13}C and D towards the sediment surface indicate that most of the CH_4 diffusing through this thick Holocene marine layer is removed by anaerobic oxidation with sulfate at the surface sediment before reaching the water. This has been reported by Overduin et al., 2015 for a site close-by.

This surface layer may also act as a physical barrier preventing gas to migrate towards the surface directly. The CH_4 concentration increase from 9 to 5.8m depth without strong isotopic shifts (Fig. 5) and the acoustic data (Fig. S3) show that gas accumulates under this relatively impermeable layer. The upward CH_4 flux is therefore highly restrained facilitating horizontal gas transport towards e.g. open taliks or hotspot locations where part of the gas can be released as bubbles to the water column without being oxidized. The isotopic signatures of the CH_4 in the pore water of the hotspot cores do not show isotopic fractionation toward the surface (Fig.2). This is likely because at these sites, ebullition processes may physically disturb the sulfate reducing layer and reduce the amount of CH_4 subject to anaerobic oxidation (only dissolved CH_4 is accessible for methanotrophic organisms).

The shallow sediment samples have ^{14}C values from 3 to 88pmC (radiocarbon age= 1-26kyBP) showing the presence of old CH_4 in surface sediment of relatively modern age and thus confirming the migration of old gas from deeper reservoir towards the surface. Note that the overall low content of organic carbon (<2.3%) with a high fraction of lignin (Bröder et al., 2016; Tesi et al., 2015; Vonk et al., 2014) in the surface sediment (Fig.5) would anyway inhibit CH_4 formation in the marine layer hence in situ methanogenesis there is highly unlikely.

3.5. CH_4 in the water

CH_4 in water samples is more enriched in heavy isotopes than in sediment samples. The highest CH_4 concentrations in the water column are observed close to the seabed and at the surface in the presence of sea ice (Fig.2a blue triangles). The ^{14}C values of water samples are between 83 and 9560pmC (radiocarbon age= 2kyBP to strongly enriched above natural

Biogeosciences Discuss., doi:10.5194/bg-2016-367, 2016
Manuscript under review for journal Biogeosciences
Published: 7 September 2016
© Author(s) 2016. CC-BY 3.0 License.

present day values) (Fig.2d) (SI section 3). For the water samples, we only encountered the highly enriched ^{14}C values at the shelf edge, but we suggest that this signature is likely diluted over the shelf, where old CH_4 from the sediment is added. This could explain the broad range of pmC values observed in the water column.

Two scenarios may explain the difference in stable isotope signatures between the water- and sediment samples. The first assumes a mixture of depleted old CH_4 from CO_2 reduction from the sediment (as identified above) with a source that is more enriched in heavy isotopes. This source could be either "in-situ" production in the water or thermal degradation of organic matter in the deep Earth layers. In the marine environment, CH_4 could in principle be produced at the pycnocline, where natural differences of water density create a "fluid bottom", on which organic particles and pellets could accumulate as substrate for "in-situ" methanogenesis (Damm et al., 2008, Karl et al., 2008, Sasakawa et al., 2008). In the ESAS, the pycnocline is very shallow and a very low primary production is expected because of darkness and ice cover in the winter and because of the little available sunlight in the summer due to the high solar zenith angles and the very turbid waters (light penetrates only down to 40cm). Water "in-situ" production of CH_4 is therefore very unlikely. Thermogenic emissions from the sediment are possible, especially from the fault zone near the shelf edge where we find strong heavy isotope enrichment in the water. We have not measured any CH_4 with a thermogenic isotopic signature in our deep sediment cores, but one should note that deep sediment drilling in the shelf edge was not possible because of the rough ice conditions.

As a second hypothesis, the isotopic signature of the water samples may also result from substantial aerobic (e.g. in the water under the sea ice) or anaerobic (in the surface sediment) oxidation of CH_4 emitted from the deep sediment. To test this quantitatively, we plotted oxidation slopes (showing the evolution of the isotopic signature of the remaining CH_4 after oxidation) for the largest and lowest fractionation factors (ε_D: 98-324‰ and ε_{13C}: 2-38‰) found in the literature (Table 1) and using the samples with the highest concentration as initial source in a dual isotope plot (Fig.4). At first sight and when using these wide ranges of fractionation factors, all water samples may be the result of CH_4 oxidation in the surface sediment or in the water. In such a case, however, the samples with the more enriched isotope signatures should correspond to the lower concentration, which is not the case, especially for the shelf edge samples that show the opposite pattern (Fig.2, yellow triangles). Oxidation alone, without the addition of CH_4 from another source, can thus not explain the stable isotope difference between the water and sediment samples.

CH_4 measured in the water samples is mainly dissolved CH_4, because of the low probability to trap bubbles in the Niskin bottles during sampling. In the sediment, gas bubbles have time to equilibrate with pore water, especially when the gas is trapped under relatively impermeable sediment, e.g. the Holocene marine silty-clay layer. Therefore, we assume that in the sediment, the pore water is in equilibrium with the gas bubbles, while we suggest that in the seawater bubbles travel too rapidly to reach an isotopic equilibrium with

Biogeosciences Discuss., doi:10.5194/bg-2016-367, 2016
Manuscript under review for journal Biogeosciences
Published: 7 September 2016
© Author(s) 2016. CC-BY 3.0 License.

the dissolved gas. This means that the CH_4 isotopic signature of the gas bubbles may not strongly affect the CH_4 dissolved in seawater. Our triple isotope observations therefore show that CH_4 dissolved in ESAS seawater likely originates for a large part from old deep gas that is only partially oxidized in the sediment surface. This gas mixes into a small background reservoir that is highly enriched in ^{14}C and causes the higher pmC values in the seawater in comparison with pore water sediment.

4. Conclusion

Our triple isotope dataset of CH_4 from the sediment and water of the ESAS reveals the presence of large amounts of biogenic CH_4 in the shelves. This gas is formed continuously from old substrates at depth and/or has been stored as gas hydrate and/or gas pockets in or below the subsea permafrost.

We show that already today this CH_4 from deep, old reservoirs migrates through the thawing permafrost towards the seafloor, either dissolved in the sediment pore water or as gas bubbles, to reach the seawater. The very shallow depth of the ESAS allows a short path for these bubbles to reach the atmosphere, and the major sea ice extent decline in this area may additionally enhance the escape to the atmosphere. No quantitative estimate of this CH_4 source is to date possible, but a rise in temperature will enhance microbial formation and permafrost thawing, hence emissions of biogenic CH_4 from the deep subsea permafrost of the ESAS are expected to play an increasingly important role for the radiative forcing of the Earth in the future.

Variations in CH_4 isotopic signatures in air trapped in polar ice cores have been studied to investigate the cause(s) of the CH_4 increase observed during past warming events (Sowers, 2006, Fischer et al., 2008, Bock et al., 2010). The authors measured a shift towards lighter CH_4 stable isotope values together with a temperature increase and they concluded that a rise in wetland CH_4 emissions is the most likely explanation. Our results show that thawing subsea permafrost emits large amounts of CH_4 that is depleted in heavy isotopes and that such emissions cannot be easily distinguished from Arctic wetland emissions when looking only at stable isotope data. Considering the sensitivity of subsea permafrost to warming, such emissions may have played a significant role in the large CH_4 rises recorded in ice core air during warming events in the past.

ACKNOWLEDGEMENTS

We are grateful to the help of Gary Salazar (University of Bern) with the ^{14}C measurements. This research was supported by the Russian Government (No. 14.Z50.31.0012/03.19.2014), the US National Science Foundation (OPP ARC-1023281; 0909546); the NOAA Climate Program office (NA08OAR4600758). N.S., D.K., and O.D. acknowledge support from the Russian Science Foundation (No. 15-17-20032).

Biogeosciences Discuss., doi:10.5194/bg-2016-367, 2016
Manuscript under review for journal Biogeosciences
Published: 7 September 2016
© Author(s) 2016. CC-BY 3.0 License.

We would like to thank Jorien Vonk, Alain Prinzhofer, Helge Niemann, Nadine Mattielli and Dominique Weiss for the fruitful discussions and precious help in the interpretation of these data and Rebecca Fisher, Elise van Winden and Joralf Quist for their help with the stable isotope measurements and system calibration.

AUTHOR CONTRIBUTION

C.J.S., N.S., T.R., J.J., S.S., I.S., J.L.T. and M.E. worked on the scientific interpretation and wrote the manuscript. N.S. and I.S. planned the research and organized the multiyear fieldwork campaigns. C.vd.V., C.J.S., S.S. and J.J. performed the isotopic analyses. I.S., D.K., O.D., V.S., A.S. and V.T. performed the water sampling, sediment drilling, the headspace preparation and CH_4 concentration measurements on the field.

REFERENCES

Alperin, M. J., Reeburgh, W. S., & Whiticar, M. J.: Carbon and hydrogen isotope fractionation resulting from anaerobic methane oxidation. Glob. Biochem. Cy., 2(3), 279-288, 1988.

Andersland, O., Ladanyi, B.: An introduction to Frozen Ground Engineering, Springer US, pp.352, 1994.

Bauch, H. A., Mueller-Lupp, T., Taldenkova, E., Spielhagen, R. F., Kassens, H., Grootes, P. M., Thiede, J., Heinemeier, J., & Petryashov, V. V.: Chronology of the Holocene transgression at the North Siberian margin. Global Planet. Change, 31, 125-139, 2001.

Bock, M., Schmitt, J., Möller, L., Spahni, R., Blunier, T., Fischer, H.: Hydrogen isotopes preclude marine hydrate CH4 emissions at the onset of Dansgaard-Oeschger events, Science, 328, 1686-1689, 2010.

Brass, M., & Röckmann, T.: Continuous-flow isotope ratio mass spectrometry method for carbon and hydrogen isotope measurements on atmospheric CH_4, Atm. Meas. Tech., 3, 1707–1721, 2010.

Bröder, L., Tesi, T., Andersson A., Eglinton T.I., Semiletov I. P., Dudarev O. V., Roos P., Gustafsson Ö. (2016), Historical records of organic matter supply and degradation status in the East Siberian Sea, *Organic Geochemistry*, Vol. 91, P. 16-30, 2016.

Brosius, L. S., Walter Anthony, K. M., Grosse, G., Chanton, J. P., Farquharson, L. M., Overduin, P. P. & Meyer, H.: Using the deuterium isotope composition of permafrost meltwater to constrain thermokarst lake

Biogeosciences Discuss., doi:10.5194/bg-2016-367, 2016
Manuscript under review for journal Biogeosciences
Published: 7 September 2016
© Author(s) 2016. CC-BY 3.0 License.

470 contributions to atmospheric CH4 during the last deglaciation. J. Geophys.
471 Res., 117, G01022, 2012.
472
473 Chanton, J. P., Fields, D., & Hines, M. E.: Controls on the hydrogen isotopic
474 composition of biogenic methane from high-latitude terrestrial wetlands. J.
475 Geophys. Res., 111, G04004, 2006.
476
477 Charkin A.N.,Dudarev O.V., Semiletov I.P., Kruhmalev A.V., Vonk J.E.,
478 Sánchez-García L., Karlsson E., and Ö. Gustafsson: Seasonal and
479 interannual variability of sedimentation and organic matter distribution in the
480 Buor Khaya Gulf – the primary recipient of input from Lena River and coastal
481 erosion in the SE Laptev Sea, Biogeosciences, 8, 2581–941, 2011.
482
483 Coleman, D. D., Risatti, J. B., & Schoell, M.: Fractionation of carbon and
484 hydrogen isotopes by methane-oxidizing bacteria. Geochim. Cosmochim.
485 Acta, 45, 1033-1037, 1981.
486
487 Damm, E., Kiene, R.P., Schwarz, J.,Falck., E & Dieckmann, G.: Methane
488 cycling in Arctic shelf water and its relationship with phytoplankton biomass
489 and DMSP, Marine Chemistry, 19, 45-59, 2008.
490
491 Dmitrenko, I. A., Kirillov, S. A., Tremblay, L. B., Kassens, H., Ansimov, O. A.,
492 Lavrov, S. A., Razumov, S. O., & Grigoriev, M. N.: Recent changes in shelf
493 hydrography in the Siberian Arctic: Potential for subsea permafrost instability.
494 J. Geophys. Res., 116, C10027, 2011.
495
496 Egger, M., Rasigraf, O., Sapart, C. J., Jilbert, T., Jetten, M. S. M., Röckmann,
497 T., van der Veen, C., Bândă, N., Kartal, B., Ettwig, K. F. and Slomp, C. P.:
498 Iron-Mediated Anaerobic Oxidation of Methane in Brackish Coastal
499 Sediments, Environ. Sci. Technol., 49(1), 277–283, 2015.
500
501 Feisthauer, S., Vogt, C., Modrzynski, J., Szlenkier, M., Krüger, M., Siegert, M.,
502 & Richnow, H.-H.: Different types of methane monooxygenases produce
503 similar carbon and hydrogen isotope fractionation patterns during methane
504 oxidation. Geochim. Cosmochim. Acta, 75, 1173-1184, 2011.
505
506 Feng, X., Vonk, J. E., van Dongen, B. E., Gustafsson, Ö., Semiletov, I. P.,
507 Dudarev, O. V., Wang, Z., Montluçon, D. B., Wacker, L., & Eglinton, T. I.:
508 Differential mobilization of terrestrial carbon pools in Eurasion Arctic river
509 basins. PNAS, 110, 14168-14173, 2013.
510
511 Fischer, H., Behrens, M., Bock, M., Richter, U., Schmitt, J., Loulergue, L.,
512 Chappellaz, J., Spahni, R., Blunier, T., Leuenberger, M., & Stocker, T. F.:
513 Changing boreal methane sources and constant biomass burning during the
514 last termination. Nature, 452, 864-867, 2008.
515

© Author(s) 2016. CC-BY 3.0 License.

Friedman, I., Redfield, A. C., Schoen, B., & Harris, J.: The Variation of the Deuterium Content of Natural Waters in the Hydrologic Cycle. Rev. of Geophys., 2(1), 177-224, 1964.

Henrichs, S. M., & Reeburgh, W. S.: Anaerobic mineralization of marine sediment organic matter: Rates and the role of anaerobic processes in the oceanic carbon economy. Geomicrobiol. J., 5, 191-237, 1987.

Holler, T., Wegener, G., Knittel, K., Boetius, A., Brunner, B., Kuypers, M. M. M., & Widdel, F.: Substantial $^{13}C/^{12}C$ and D/H fractionation during anaerobic oxidation of methane by marine consortia enriched in vitro. Environ. Microbiol. Rep., 1, 370-376, 2009.

IPCC, 2013: *Climate Change 2013: The Physical Science Basis. Contribution of Working Group I to the Fifth Assessment Report of the Intergovernmental Panel on Climate Change* [Stocker, T.F., D. Qin, G.-K. Plattner, M. Tignor, S.K. Allen, J. Boschung, A. Nauels, Y. Xia, V. Bex and P.M. Midgley (eds.)]. Cambridge University Press, Cambridge, United Kingdom and New York, NY, USA, 1535 pp, 2013.

James, R. H., Bousquet, P., Bussmann, I., Haeckel, M., Kipfer, R., Leifer, I., Niemann, H., Ostrovsky, I., Piskozub, J., Rehder, G., Treude, T., Vielstädte, L. and Greinert, J.: Effects of climate change on methane emissions from seafloor sediments in the Arctic Ocean: A review. Limnol. Oceanogr, special issue,2016.

Karl, D.M., Beversdorf, L., Bjorkman, K.M., Church, M.J., Martinez, A. & Delong, E.F.: Aerobic production of methane in the sea, Nature Geoscience, 1, 473-478, 2008.

Karlsson, E. S., Charkin, A., Dudarev, O. Semiletov, I. P., Vonk, J. E., Sánchez-García, L., Andersson, A., and Gustafsson, Ö.: Carbon isotopes and lipid biomarker investigation of sources, transport and degradation of terrestrial organic matter in the Buor-Khaya Bay, SE Laptev Sea, Biogeosciences, 8, 1865-1879, 2011.

Karlsson, E., Gelting, J., Tesi, T., Van Dongen, B., Andersson, A., Semiletov, I.,…, and Gustafsson, Ö: Different sources and degradation state of dissolved, particulate, and sedimentary organic matter along the Eurasian Arctic coastal margin. Global Biogeochemical Cycles, 30(6), 898–919, 2016

Keeling, C. D.: The concentration and isotopic abundances of carbon dioxide in rural and marine air. Geochim. Cosmochim. Acta, 24, 277-298,1961.

Kessler, J. D., Reeburgh, W. S., & Tyler, S. C.: Controls on the methane concentration and stable isotope (δ^2H-CH_4 and δ^{13}C-CH_4) distribution in the water columns of the Black Sea and Cariaco Basin. Glob. Biogeochem. Cy., 20, GB4004, 2006.

© Author(s) 2016. CC-BY 3.0 License.

564
565 Kessler, J. D. et al. A persistent oxygen anomaly reveals the fate of spilled
566 methane in the deep Gulf of Mexico. Science, 331, 312–315, 2011.
567
568 Kinnaman, F. S., Valentine, D. L., & Tyler, S. C.: Carbon and hydrogen
569 isotope fractionation associated with the aerobic microbial oxidation of
570 methane, ethane, propane and butane. Geochim. Cosmochim. Acta, 71, 271-
571 283, 2007.
572
573 Knittel, K.; Boetius, A. Anaerobic oxidation of methane: Progress with an
574 unknown process. Annu. Rev. Microbiol., 63, 311–334, 2009.
575
576 Kvenvolden, K. A.: Methane hydrates and global climate. Glob. Biogeochem.
577 Cy., 2(3), 221–229, 1988.
578
579 Lammers, S., Suess, E.: An improved head-space analysis method for
580 methane in seawater, Marine Chemistry 47, 115-125, 1994.
581
582 Lessner, D. J.: Methanogenesis Biochemistry. In: Encyclopedia of Life
583 Sciences (ELS). Chichester, UK: Wiley and Sons Ltd, 2009.
584
585 Martens, C. S., Albert, D. B., & Alperin, M. J.: Stable isotope tracing of
586 anaerobic methane oxidation in the gassy sediments of Eckernförde Bay,
587 German Baltic Sea. Am. J. Sci., 299, 589-610, 1999.
588
589 Mau, S., Blees, J., Helmke, E., Niemann, H. & Damm, E. Vertical distribution
590 of methane oxidation and methanotrophic response to elevated methane
591 concentrations in stratified waters of the Arctic fjord Storfjorden (Svalbard,
592 Norway). Biogeosciences, 10 6267–6278, 2013.
593
594 Nicolsky, D., Romanovsky, V. E., Romanovskii, N. N., Kholodov, A. L.,
595 Shakhova, N. E., & Semiletov, I. P.: Modeling sub-sea permafrost in the East
596 Siberian Arctic Shelf: The Laptev Sea region. J. Geophys. Res., 117, F03028,
597 2012.
598
599 O'Connor, F. M., Boucher, O., edney, N., ones, C. D., Folberth, . A., Coppell,
600 R., Friedlingstein, P., Collins, W. J., Chappellaz, J., Ridley, J., & Johnson, C.
601 E.: Possible role of wetlands, permafrost and methane hydrates under future
602 climate change: a review. Rev. Geophys., 48, RG4005, 2010.
603
604 Overduin, P. P., S. Liebner, C. Knoblauch, F. Günther, S. Wetterich, L.
605 Schirrmeister, H.-W. Hubberten, & M. N. Grigoriev: Methane oxidation
606 following submarine permafrost degradation: Measurements from a central
607 Laptev Sea shelf borehole, J. Geophys. Res. Biogeosci., 120,965–978,
608 doi:10.1002/2014JG002862, 2015.
609

© Author(s) 2016. CC-BY 3.0 License.

610 Quay, P., Stutsman, J., Wilbur, D., Snover, A., Dlugokencky, E. J., & Brown,
611 T.: The isotopic composition of atmospheric CH4. Glob. Biogeochem. Cy., 13,
612 445-461, 1999.
613
614 Rasigraf, O., Vogt, C., Richnow, H.-H., Jetten, M. S. M., & Ettwig, K. F.:
615 Carbon and hydrogen isotope fractionation during nitrite-dependent anaerobic
616 methane oxidation by Methylomirabilis oxyfera. Geochim. Cosmochim. Acta,
617 89, 256-264, 2012.
618
619 Romanovskii, N. N., Hubberten, H.-W., Gavrilov, A. V., Eliseeva, A. A., &
620 Tipenko, G. S.: Offshore permafrost and gas hydrate stability zone on the
621 shelf of East Siberian Seas. Geo-Mar. Lett., 25, 167-182, 2005.
622
623 Reeburgh, W. S., Tyler, S. C., & Carroll, J.: Stable carbon and hydrogen
624 isotope mesurements on Black Sea water-column methane. Deep-Sea Res. II,
625 53, 1893-1900, 2006.
626
627 Reeburgh, W. S. Oceanic methane biogeochemistry. Chem. Rev. 2007, 107,
628 486–513.
629
630 Ruff, M., Szidat, S., Gäggeler, H. W., Suter, M., Synal, H.-A., & Wacker, L.:
631 Gaseous radiocarbon measurements of small samples, Nucl. Instr. and Meth.
632 B, 268, 790-794, 2010.
633
634 Sapart, C. J., van der Veen, C., Vigano, I., Brass, M., van de Wal, R. S. W.,
635 Bock, M., Fischer, H., Sowers, T., ... Röckmann, T. (2011). Simultaneous
636 stable isotope analysis of methane and nitrous oxide on ice core samples.
637 Atm. Meas. Tech., 4, 2607- 2618.
638
639 Sasakawa, M., Tsunogai, U., Kameyama,S., Nakagawa, F., Nojiri, Y. and
640 Tsuda, A.: Carbon isotopic characterization for the origin of excess methane
641 in subsurface seawater, Journal of Geophysical Research, 113, CO3012,
642 2008.
643
644 Semiletov I.P., Pipko I.I., Shakhova N.E., Dudarev O.V., Pugach S.P.,
645 Charkin A.N., McRoy C.P., Kosmach D., and Gustafsson, Ö.: Carbon
646 transport by the Lena River from its headwaters to the Arctic Ocean, with
647 emphasis on fluvial input of terrestrial particulate organic carbon vs. carbon
648 transport by coastal erosion, Biogeosciences, 8, 2407-2426, 2011.
649
650 Semiletov I.P., Shakhova N. E., Sergienko V.I., Pipko I.I., and O. Dudarev:
651 On Carbon Transport and Fate in the East Siberian Arctic Land-Shelf-
652 Atmosphere System, Environment Research Letters, 7, 2012.
653
654 Schmitt, M., Faber, E., Botz, R., and Stoffers, P.: Extraction of methane from
655 seawater using ultrasonic vacuum degassing, Anal. Chemistry 63, vol. 5, 529-
656 532, 1991.
657

© Author(s) 2016. CC-BY 3.0 License.

Schoell, M.: Multiple origins of methane on Earth. Chemical Geology, 71, 1-10, 1988.

Schuur, E.A.G., Abbott, B. W., Bowden, W. B., Brovkin, V., Camill, P., Canadell,…. and Zimov, S. A.: Expert assessment of vulnerability of permafrost carbon to climate change. Climatic Change, 119(2), 359-374, 2013.

Shakhova, N., I. Semiletov, and G. Panteleev: The distribution of methane on the Siberian Arctic shelves: Implications for the marine methane cycle, Geophysical Research Letters, 32, L09601, 2005.

Shakhova N.E., Nicolsky D., and I. P. Semiletov: On the current state of sub-sea permafrost in the East-Siberian Shelf testing of modeling results by observational data. *Transactions of Russian Academy of Sciences, Vol. 429 (5)*, 2009 (translated in English by Springer), 2009.

Shakhova, N., Semiletov, I., Leifer, I., Rekant, P., Salyuk, A., & Kosmach, D. Geochemical and geophysical evidence of methane release from the inner East Siberian Shelf. J. Geophys. Res., 115, C08007, 2010a.

Shakhova, N, I. Semiletov, A. Salyuk, V. Yusupov, D. Kosmach & O. Gustafsson: Extensive methane venting to the atmosphere from sediments of the East Siberian Arctic Shelf, Science, 327, 1246-1250, 2010b.

Shakhova, N., Semiletov, I., Leifer, I., , Sergienko, V., Salyuk, A., Kosmach, D., Chernikh D., Stubbs Ch., Nicolsky D., Tumskoy V., and O. Gustafsson Ebullition and storm-induced methane release from the East Siberian Arctic Shelf, Nature Geosciences, vol.7, No.1, 64-70, 2014.

Shakhova N., Semiletov, I., Sergienko, V., Lobkovsky, L., Yusupov, V., Salyuk, A., Salomatin, A., Chernykh, D., Kosmach, D., Panteleev, G., Nicolsky, D., Samarkin, V., Joye, S., Charkin, A., Dudarev, O., Meluzov, A., Gustafsson, O.: The East Siberian Arctic Shelf: towards further assessment of permafrost-related methane fluxes and role of sea ice. Phil. Trans. R. Soc. A, vol. 373: 20140451, 2015.

Sloan, E. D.: Fundamental principles and applications of natural gas hydrates. Nature, 426, 353-359, 2003.

Soloviev, V. A., Ginzburg, G. D., Telepnev, E. V., & Mikhaluk, Y. N.: Cryothermia and gas hydrates in the Arctic Ocean. Leningrad: Sevmorgeologia, 1987.

Sowers, T.: Late quaternary atmospheric CH4 isotope record suggests marine clathrates are stable. Science, 311, 838-840, 2006.

© Author(s) 2016. CC-BY 3.0 License.

Steinle, L, Graves, C., Treude, T., Ferré, B., Biastoch, A., Bussmann, I., Berndt, C., Krastel, S., James, R.H., Behrens, E., Böning, C.W., Greinert, J., Sapart, C.J., Scheinert, M., Sommer, S., Lehmann, M.F. and Niemann, H.: Water column methanotrophy controller by a rapod oceanographic switch. Nature Geoscience, 8, 378-382, 2015.

Szidat, S., Salazar, G. A., Vogel, E, Battaglia, M., Wacker, L., Synal, H.-A. and Türler, A.: 14C analysis and sample preparation at the new Bern Laboratory for the analysis of radiocarbon with AMS (LARA), Radiocarbon, 56, 561-566, 2014.

Tesi, T., Semiletov, I., Hugelius, G., Dudarev, O., Kuhry, P., and Gustafsson, Ö.: Composition and fate of terrigenous organic matter along the Arctic land–ocean continuum in East Siberia: Insights from biomarkers and carbon isotopes, Geochimica et Cosmochimica Acta, 133, 235–256, 2014.

Tesi, T., I. Semiletov, O. Dudarev, A. Andersson, and Ö. Gustafsson: Matrix association effects on hydrodynamic sorting and degradation of terrestrial organic matter during cross-shelf transport in the Laptev and East Siberian shelf seas, J. Geophys. Res. Biogeosci., 121, 2016.

Vonk, J. E., Sánchez-García, L., van Dongen, B. E., Alling, V., Kosmach, D., Charkin, A., Semiletov, I. P., Dudarev, O. V., Shakhova, N., Roos, P., Eglinton, T. I., Andersson, A., & Gustafsson, Ö.: Activation of old carbon by erosion of coastal and subsea permafrost in Arctic Siberia. Nature, 489, 137–140, 2012.

Vonk J.E., Semiletov, I.P., Dudarev O.V., Eglinton T.I., Andersson A., Shakhova N., Charkin A., Heim B., Gustafsson: Preferential burial of permafrost derived organic carbon in Siberian-Arctic shelf waters, J. Geophys. Res., Vol. 119, N 12, P. 8410-8421, 2014.

Wiesenburg, D. A., & Guinasso Jr., N. L. (1979). Equilibrium solubilities of methane, carbon monoxide and hydrogen in salt and sea water. J. Chem. Eng. Data, 24(4), 356-360.

Whiticar, M. J., & Faber, E.: Methane oxidation in sediment and water column 20120environments – Isotope evidence. Org. Geochem., 10, 759-768, 1986.

Whiticar, M. J.: Carbon and hydrogen isotope systematics of bacterial formation and oxidation of methane. Chem. Geo., 161, 291-314, 1999.

Biogeosciences Discuss., doi:10.5194/bg-2016-367, 2016
Manuscript under review for journal Biogeosciences
Published: 7 September 2016
© Author(s) 2016. CC-BY 3.0 License.

765 # Table and Figures

766

Processes	ε (^{13}C) (‰)	ε (D) (‰)
Anaerobic Methane Oxidation		
Marine sediment and water column (Whiticar and Faber, 1986)	**2 - 14**	
Marine sediment – Baltic Sea (Martens et al., 1999)	**11 - 13**	**100 - 140**
Brackish/marine sediment – Bothnian Sea (Egger et al., 2015)	**9**	**98**
Marine sediments – Alaska (Alperin et al., 1988)	**8 - 10**	**134 - 180**
Marine sediment - Hydrate Ridge, Pacific Ocean (Holler et al., 2009)	**12**	**105 - 156**
Marine sediment - Mud Volcano, Mediterranean Sea (Holler et al., 2009)	**19 - 23**	**139 - 185**
Microbial mat – Black Sea (Holler et al., 2009)	**34 - 38**	**273 - 324**
Water column – Black Sea (Reeburgh et al. 2006)	**16 - 24**	
Water column – Black Sea, Cariacco Basin (Kessler et al., 2006)	**20 - 22**	**181 - 221**
Incubation, nitrite-driven AOM (Rasigraf et al., 2012)	**27 - 32**	**272 - 317**
Aerobic Methane Oxidation		
Seep field offshore CA, USA (Kinnaman et al., 2007)	**22 - 30**	**156 - 320**
Laboratory incubation (Coleman et al., 1981)	**13 - 25**	**97 - 350**
Laboratory incubation (Feisthauer et al., 2011)	**15 - 28**	**110 - 232**

767 **Table 1: Literature review of the fractionation factor ε associated with CH_4 oxidation in the marine**
768 **environment.**

769

770

Biogeosciences Discuss., doi:10.5194/bg-2016-367, 2016
Manuscript under review for journal Biogeosciences
Published: 7 September 2016
© Author(s) 2016. CC-BY 3.0 License.

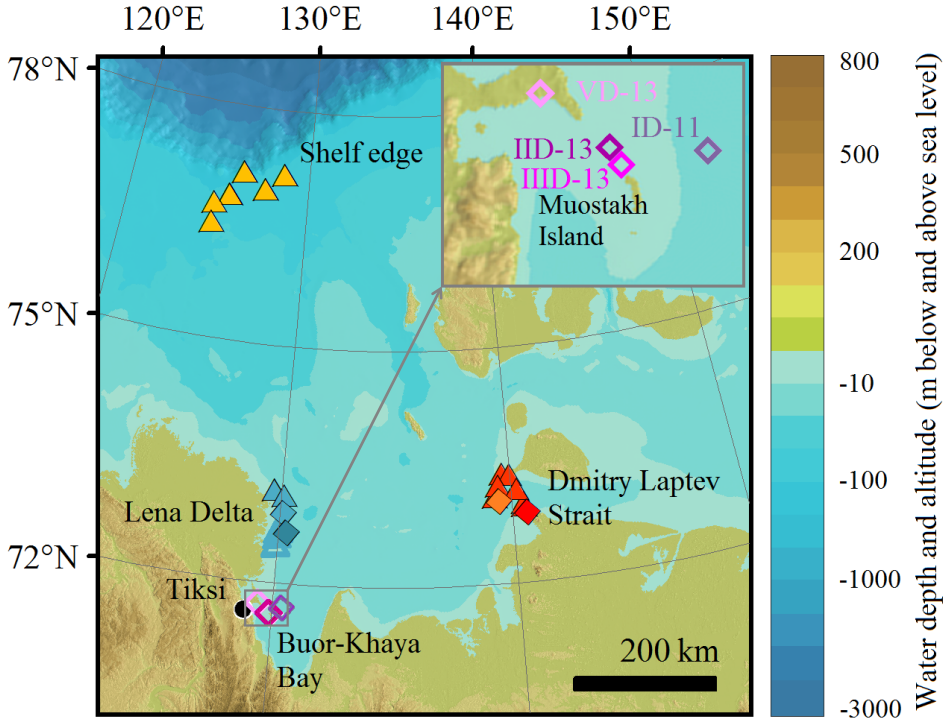

Figure 1: Sampling location. Water sampling (triangles), sediment drilling (diamonds). Summer sampling (close symbols) and winter sampling (open symbols). The color legends of the deep sediment cores are shown on the top right.

Biogeosciences Discuss., doi:10.5194/bg-2016-367, 2016
Manuscript under review for journal Biogeosciences
Published: 7 September 2016
© Author(s) 2016. CC-BY 3.0 License.

776

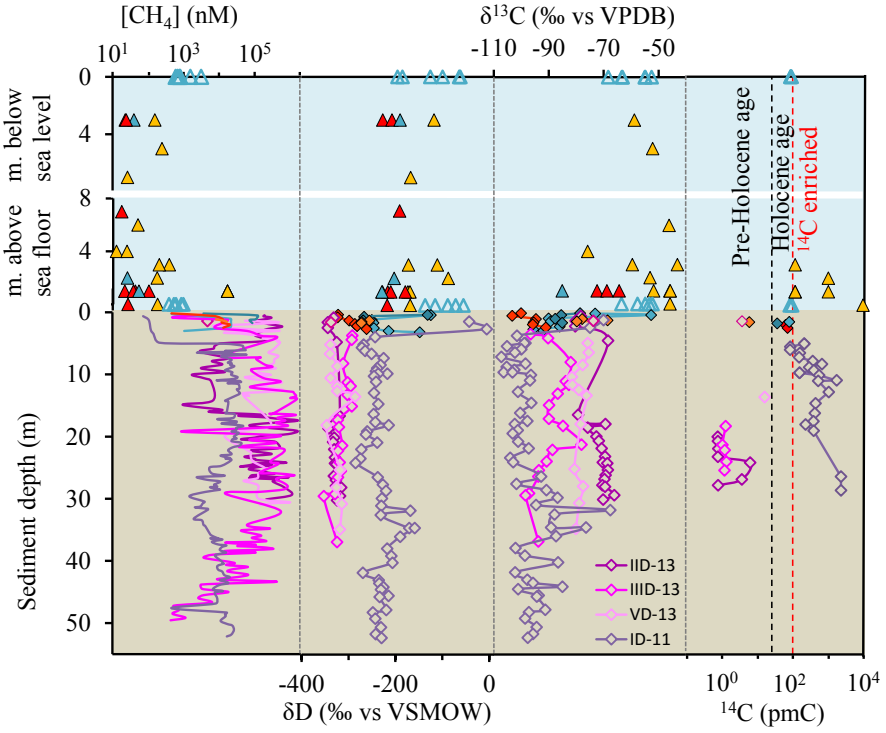

777
778 **Figure 2: CH_4 data from sediment and overlying water sampled at the East Siberian Arctic Shelf.**
779 **Water sampling (triangles), sediment cores (diamonds). Summer sampling (close symbols) and**
780 **winter sampling (open symbols). Buor Khaya Bay (purple, ID-11: background site and IID-13, IIID-**
781 **13 and VD13 hotspot sites), Dmitry Laptev Strait (red and orange), Lena Delta (light blue) and Shelf**
782 **Edge (yellow) (see Fig.1 for detailed location). (a) CH_4 concentrations, (b) δD (‰ vs VSMOW), (c)**
783 **$\delta^{13}C$ (‰ vs VPDB), (d) ^{14}C (pmC). The red dotted line corresponds to modern values (i.e., 100pmC)**
784 **and the black dashed line corresponds to the onset of the Holocene (11,000 years BP). Note that y-**
785 **axis for the water samples is divided in two sections. The upper part corresponds to the depth from**
786 **the sea surface and the lower part corresponds to the depth from the seabed.**

Biogeosciences Discuss., doi:10.5194/bg-2016-367, 2016
Manuscript under review for journal Biogeosciences
Published: 7 September 2016
© Author(s) 2016. CC-BY 3.0 License.

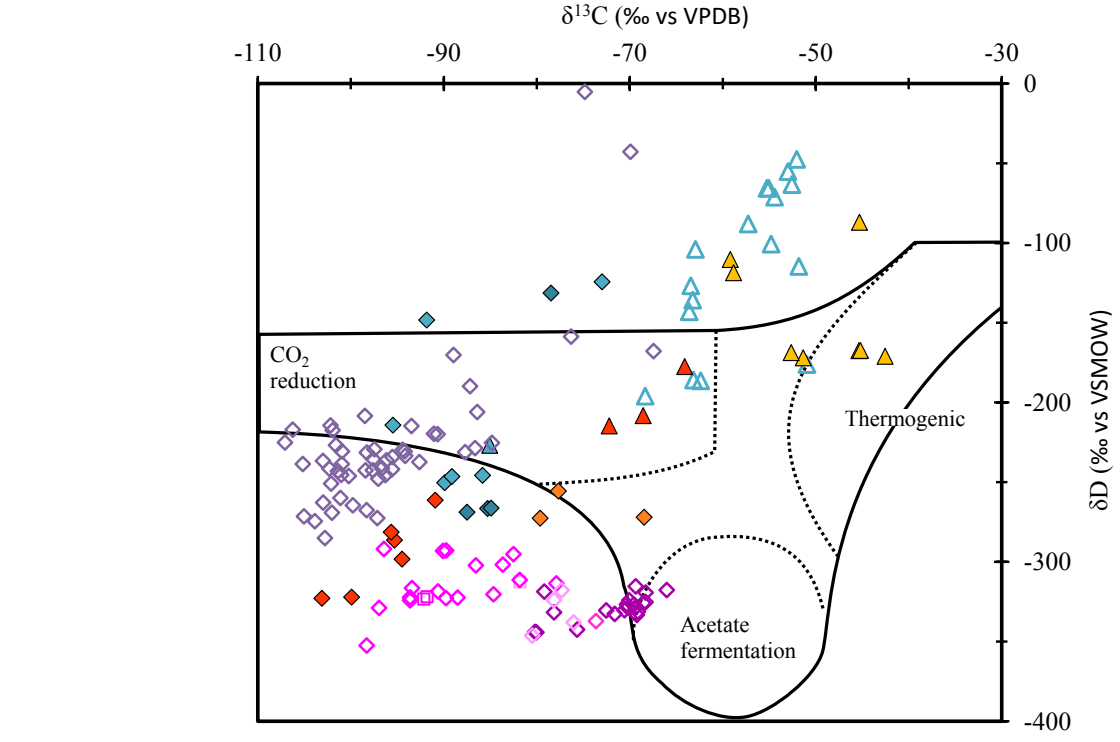

787

788 **Figure 3: Dual-isotope CH_4 plot. Legend is similar to Fig.2. Squares correspond to sample extracted**
789 **directly from porewater in the sediment. Areas delimited by black lines correspond to the three**
790 **main CH_4 formation processes and their isotopic signatures are retrieved from Whiticar, 1999.**

791
792
793
794
795
796
797
798
799
800
801
802
803
804
805
806
807
808
809
810

Biogeosciences Discuss., doi:10.5194/bg-2016-367, 2016
Manuscript under review for journal Biogeosciences
Published: 7 September 2016
© Author(s) 2016. CC-BY 3.0 License.

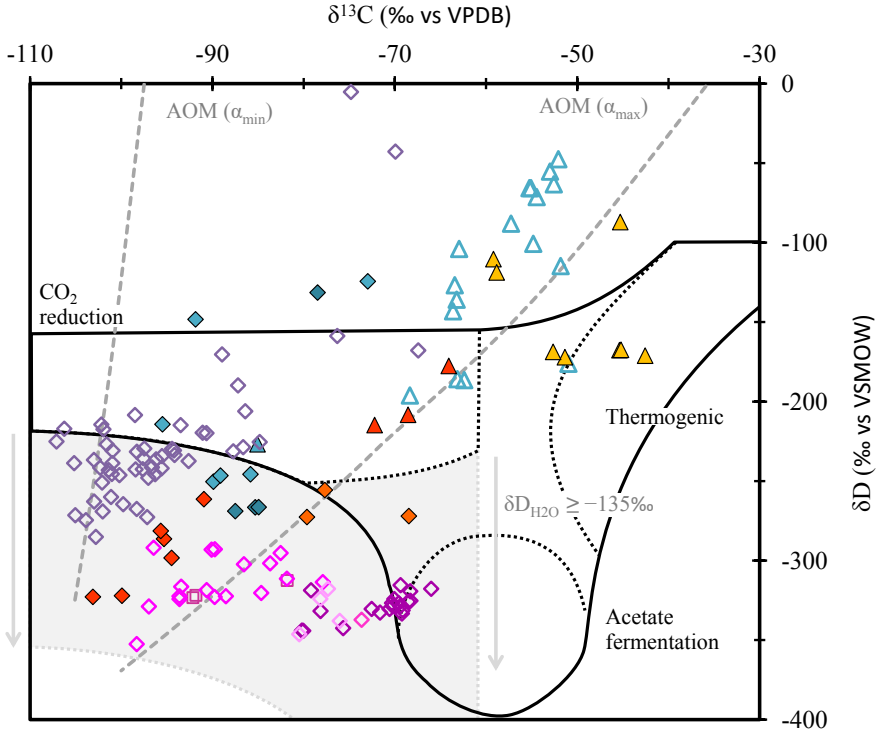

811 **Figure 4: Dual isotope plot for the CH_4 samples from the ESAS area. Water sampling (triangles),**
812 **sediment cores (diamonds). Summer sampling (close symbols) and winter sampling (open symbols).**
813 **Buor Khaya Bay (purple, ID-11: background site and IID-13, IIID-13 and VD13 hotspot sites), Dmitry**
814 **Laptev Strait (red and orange), Lena Delta (light blue) and Shelf Edge (yellow) (see Fig.1 for detailed**
815 **locations). Squares correspond to sample extracted directly from porewater in the sediment. Areas**
816 **delimited by black lines correspond to the three main CH_4 formation processes and their isotopic**
817 **signatures are retrieved from Whiticar, 1999. The shaded grey zone represents the possible CH_4**
818 **isotope signature associated to CO_2 reduction using old glacial water as substrate. Grey dashed lines**
819 **indicate oxidation slopes.**

Biogeosciences Discuss., doi:10.5194/bg-2016-367, 2016
Manuscript under review for journal Biogeosciences
Published: 7 September 2016
© Author(s) 2016. CC-BY 3.0 License.

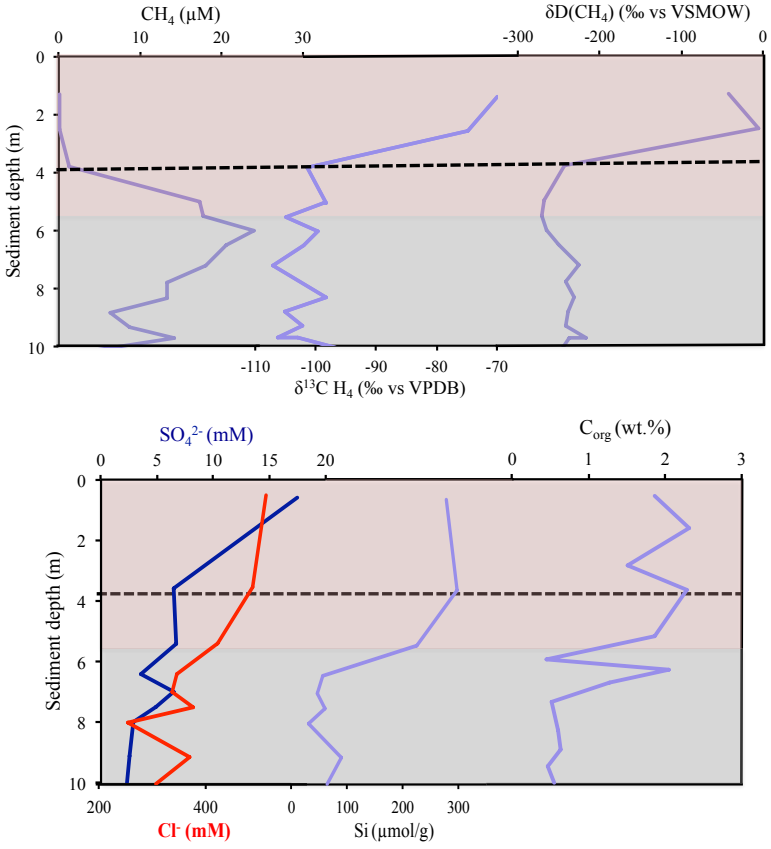

Figure 5: Close-up of the CH_4 concentration, stable isotope and other biogeochemical data of the surface of the background sediment core ID-11. Red shaded area corresponds to the marine sediment deposited during the Holocene transgression and the grey shaded area corresponds to the thawed permafrost layer. The black dotted line corresponds to the depth where CH_4 oxidation starts to occur.